International Journal of GEOMATE, March, 2022, Vol.22, Issue 91, pp.22-29
ISSN: 2186-2982 (P), 2186-2990 (O), Japan, DOI: https://doi.org/10.21660/2022.91.gxi305
Geotechnique, Construction Materials and Environment

MID-INFRARED SPECTRA OF CHLORIDE ION IMMOBILIZED ON CEMENT

Yu Hashimoto [1], *Shinichiro Okazaki[2], Kenji Wada[3], Ichiro Ishimaru[2] and Koji Kanasaki[5]

[1]Graduate School of Engineering, Kagawa University, Japan;
[2] Faculty of Engineering and Design, Kagawa University, Japan;
[3]Faculty of Medicine, Kagawa University, Japan;[5]Nisshin Kikai Co., Ltd., Japan

*Corresponding Author, Received: 22 Oct. 2021, Revised: 15 Dec. 2021, Accepted: 25 Jan. 2022

ABSTRACT: A strategy based on infrared spectroscopy is prospected to be used as a novel nondestructive inspection method to assess the risk of chloride attack on reinforced concrete (RC) structures. The characteristics of the infrared spectra of bound chloride ions in cement in the mid-infrared region were investigated in this study to examine the concentration of chloride ions on the surface of the concrete using the mid-infrared spectroscopic camera. The reflection FTIR technique was used to measure the infrared spectra of cement paste samples with varying chloride ion concentrations. Furthermore, multivariate statistical methods were applied to the obtained mid-infrared spectra to critically examine the wavelength bands of the peaks with characteristic values reflecting differences in chloride ion concentrations. As a result, if we can develop an instrument that can measure around 7300 nm, the wavelength that reflects the difference in chloride ion concentration maybe around 7300 nm.

Keywords: Mid-infrared spectroscopy, Infrared spectrum, Bound chloride ions in cement

1. INTRODUCTION

In recent years, various fields have made efforts to realize a sustainable society as outlined in the Sustainable Development Goals. For example, in civil engineering, infrastructures are being shifted from breakdown maintenance to preventive maintenance management to improve sustainability. In addition, various nondestructive testing methods have been developed in recent years and are actually in operation in the field.

Reinforced concrete is frequently used for the construction of infrastructure. When the sea breeze carries in chloride, it enters the concrete through cracks. When this chloride reaches the steel bars, corrosion begins, and the structure's life is cut short. To assess the degree of chloride deterioration of reinforced concrete, the chloride ion concentration at the location of the reinforcing bar must be measured, and a formula has been proposed to estimate the internal chloride ion concentration by measuring the concentration on the concrete surface [1][2].

With the establishment of the formula for calculating the internal chloride ion concentration, it became possible to predict the concentration at the bar's location by measuring the surface chloride ion concentration. Thus, focusing on measuring the concentration on the concrete surface, a method for estimating the concentration using near-infrared spectroscopy was proposed [3]. As a result of this study, it was found that there is a peak in the near-infrared spectrum around 2,266 nm that correlates with chloride ion concentration [3]. Based on these findings, various near-infrared spectrometers have been developed [4–7] and tested, but it has been noted that sunlight may interfere with outdoor measurements [8].

The authors have elemental technology related to a lightweight, compact, and vibration-resistant spectrometer (Fig. 1, hereinafter referred to as the "compact device") [9] that uses imaging 2-D Fourier spectroscopy in the mid-infrared region, which is less affected by low solar radiation. The size of the compact device is about 12 cm × 10 cm × 5 cm, and it weighs about 97 g. The compact device is about 12 cm × 10 cm × 5 cm in size and weighs 97 g. Therefore, it can be mounted on a drone for remote measurement in the future. Therefore, the purpose of this study is to investigate in detail the wavelengths that are correlated with the concentration of chloride ion immobilized on cement in the mid-infrared region, assuming that this device will be used, and to obtain information that will help with future measurements using this device.

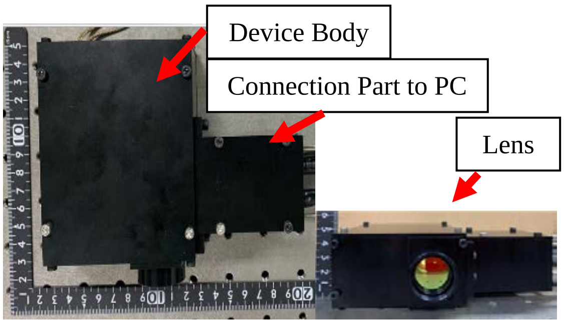

Fig.1 Spectrometer using imaging two-dimensional Fourier Spectroscopy (Compact Device)

2. INFRARED SPECTROSCOPY

Infrared spectroscopy is a spectroscopic method based on absorption, diffuse reflection, and emission of light in the infrared wavelength range. When a material is irradiated with infrared light, the molecules that make up the material absorb the light energy, causing a state transition in molecular motion. The energy of the infrared light transmitted or reflected from the material is smaller than that of the irradiated infrared light used for the state transition of molecular motion. This energy is called absorbance, and it is excellent for identifying chemical substances because each molecular structure exhibits a unique waveform. The advantages of this measurement method include the fact that it is non-destructive and non-contact and that no pretreatment is required because no chemicals are needed. In addition, the measurement time is short, which makes it easy even when the number of test pieces is large.

3. EXPERIMENTAL METHOD

3.1 Overview of Device and Measurement Methods

In this experiment, the powdered samples were measured using Fourier Transform Infrared Spectrometer (hereafter, this is called "FTIR"). In this study, the diffuse reflection method was used for the measurement. To examine the results in more detail, the number of integrations was 64 times. The FTIR-4200 type A spectrometer manufactured by JASCO Co. was used for the measurement.

3.2 Samples

Ordinary Portland cement was used to prepare the samples, and the weight ratio of water to cement (W/C) was 50%. And we mixed chlorides into each sample at 0,1,2,3,5,10,20,30 kg/m^3. Two samples were prepared, one for FTIR and the other for later measurement by the Compact Device. The samples were placed in sample forms to a height of 5cm, cured for 24 hours, and then de-molded and sealed for 21 days. After curing for 24 hours, the sample was unmolded and sealed and cured for 21 days. The reason for using a 5cm sample was to facilitate measurement with the Compact Device. After the curing was completed (Fig.2), the samples were first crushed by drilling, and then the samples were powdered in a metal mortar for FTIR analysis (Fig.2). Although it has been confirmed that the mid-infrared region is affected by moisture, we did not completely dry the powder because it might change the physical properties.

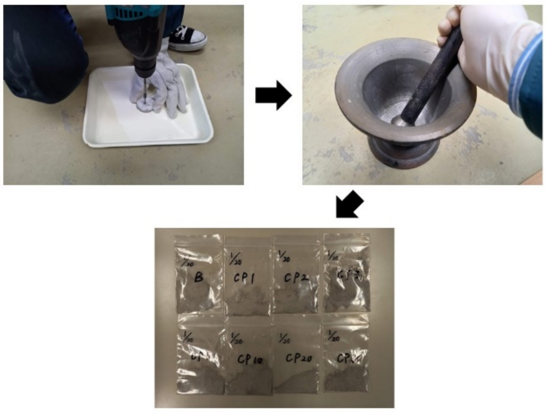

Fig.2 Powdering process of the samples

4. ANALYSIS

4.1 Spectral Processing

To improve the analytical accuracy of instrumental analysis, it is necessary to remove disturbances other than the actual information that inevitably enters the analysis as much as possible. In infrared spectroscopy, environmental factors such as fluctuations in the light source and humidity at the time of measurement often cause the entire absorption spectrum to rise and fall. This is called baseline shift, and it makes it challenging to detect apparent differences. Therefore, Standard Normal Variate (hereinafter referred to as the "SNV") is often used [10]. Let y (v, p) be the dataset of acquired spectral $y(v)$. If the spectral variable in the p-th spectral is v, the mean value of the spectral is $\bar{y}\,(p)$, and the standard deviation is $\sigma(p)$, then SNV is expressed as

$$\boldsymbol{y_{SNV}(v,p)} = \frac{\boldsymbol{y(v,p)-\bar{y}(p)}}{\boldsymbol{\sigma(p)}} \qquad (1)$$

Since this process unifies the baseline of all spectral data and makes it easier to detect apparent differences, the processed data were used in the analysis.

4.2 Analysis Methods

Multivariate analysis is used to detect apparent differences, particularly, principal component regression, and partial least squares regression analyses are often used in infrared spectroscopy [10]. In this study, these two types of analysis methods were used. The analysis was performed in the range of 5000-17000 nm, including the Compact Device's wavelength range. The Unscrambler X from Camo Analytics Co. was used for the analysis.

4.2.1 Principal component regression analysis（PCR)

In principal component regression analysis (hereinafter referred to as the "PCR"), the amount of chloride is calculated from spectral data X using the coefficient of principal component T, which is estimated to maximize the variance of X by an information compression method known as principal component analysis and by creating a regression equation using least-squares regression. The following equation expresses the model equation for principal component analysis with the weight P assigned to each wavelength:

$$X = TP^t \tag{2}$$

The superscript t represents the transpose matrix. For least-squares regression, the target variable is only the amount of chloride, so it is a simple regression. If the amount of chloride is y, the regression coefficient is q, the initial value is f; least-squares regression is expressed by the following equation, which is calculated to estimate the amount of chloride.

$$y = Tq + f \tag{3}$$

4.2.2 Partial least squares regression analysis (PLSR)

In partial least squares regression analysis (hereinafter referred to as the "PLSR"), the principal component T is calculated to optimize the covariance between the spectral data X and the amount of chloride y. Thus, the model equation is E for the residual of X, q for the coefficient of the principal component, and f for the residual of y.

$$X = TP^t + E \tag{4}$$
$$y = Tq + f \tag{5}$$

The principal component T is calculated from Eq. (4) and Eq. (5). The chloride content is estimated from Eq. (5)

5. MEASUREMENT RESULTS

In the FTIR measurement results, each spectrum is shifted up and down, making it challenging to detect characteristic differences (Fig.3). However, by using SNV, the baseline is aligned, making it easier to see the characteristic differences in the spectra (Fig.4).

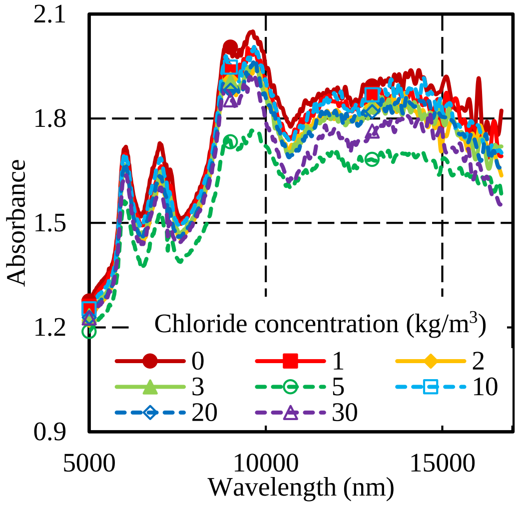

Fig.3 Original spectral data acquired by FTIR

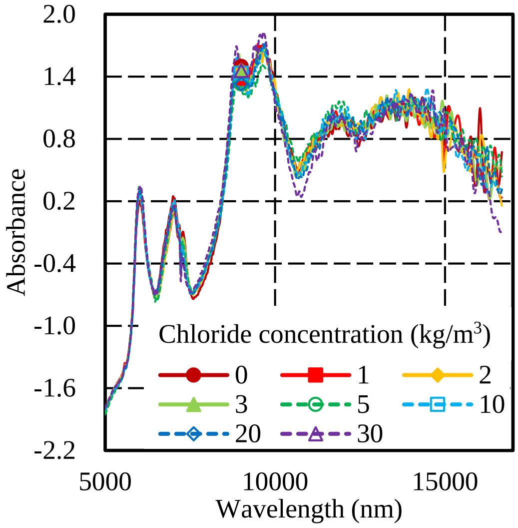

Fig.4 Spectral data acquired by FTIR after SNV processing.

6. ANALYSIS RESULTS

PLSR and PCR generated the regression equations, and the mean squared errors of the predictions of chloride concentrations were compared. The PLSR results showed a smaller mean square error than the PCR results, and the distinctive wavelengths were identified from the PLSR results.

First, comparing the predicted values based on the regression equation and the initial chloride concentration shows that the prediction is highly accurate (Fig.5). In addition, the factor contribution rate of this regression equation exceeds 70% at the third principal component (Fig.6).

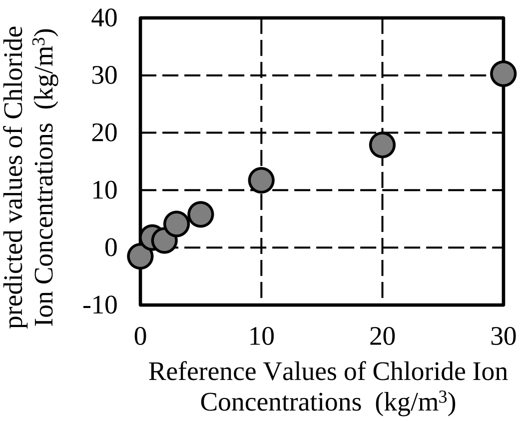

Fig.5 Comparison of standard and predicted chloride concentrations

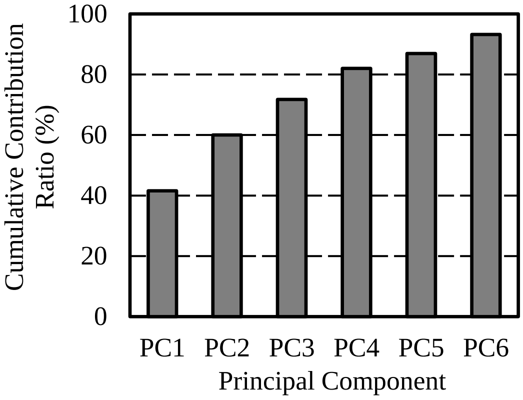

Fig.6 Cumulative contribution ratio of principal components

From Fig.6, it can be said that there is a characteristic difference in the wavelengths with large absolute values of loading among the first to third principal components. The wavelengths with particularly large absolute values are 7300, 8800, 9200, 10700, 15000, and 16300 nm (Fig.7, 8, and 9).

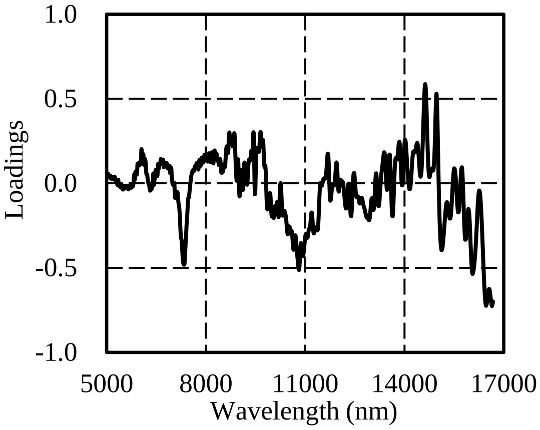

Fig.7 Loading of the first principal component

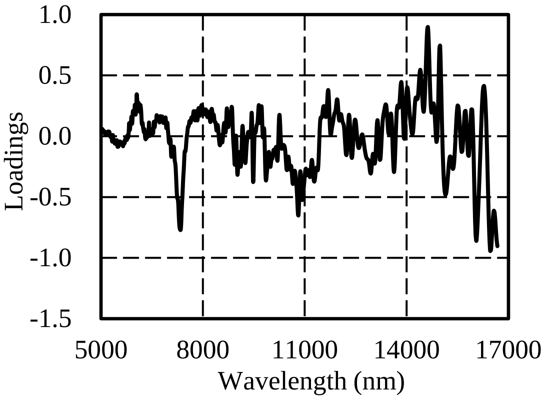

Fig.8 Loading of the second principal component

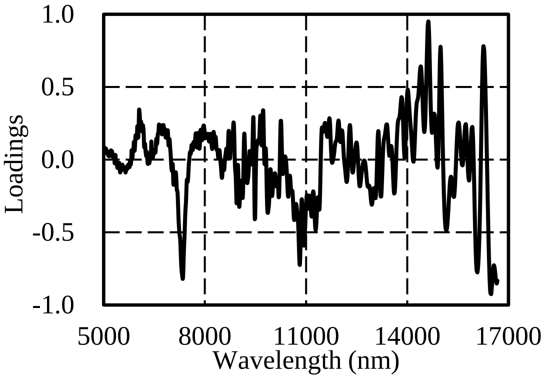

Fig.9 Loading of the third principal component

7. DISCUSSION OF ANALYSIS RESULTS

By comparing the spectra of the analysis results and the spectra after SNV processing, we will examine in detail where the wavelengths that reflect the differences in chloride concentrations are located. First, a zoomed-in view of the wavelengths with large absolute values of loading is shown (Fig.10-15).

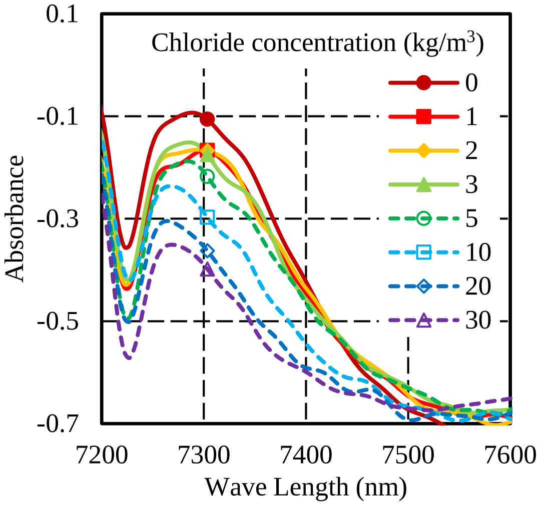

Fig.10 Absorbance data around 7300 nm

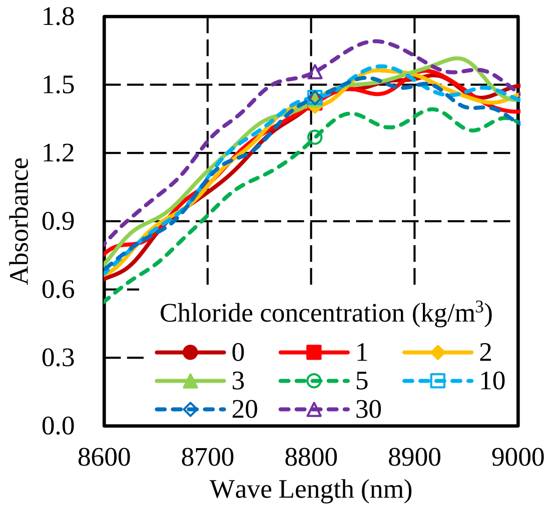

Fig.11 Absorbance data around 8800 nm

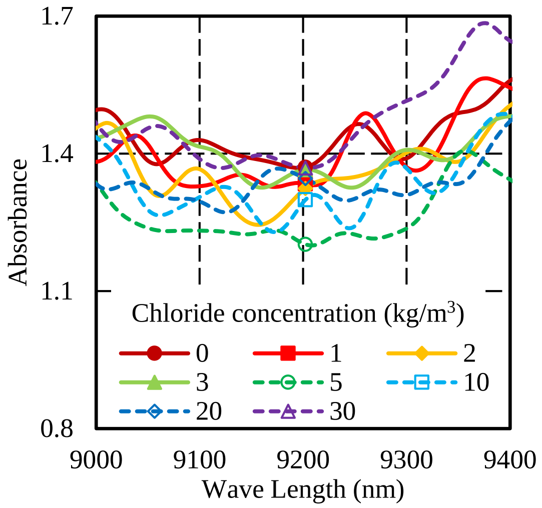

Fig.12 Absorbance data around 9200 nm

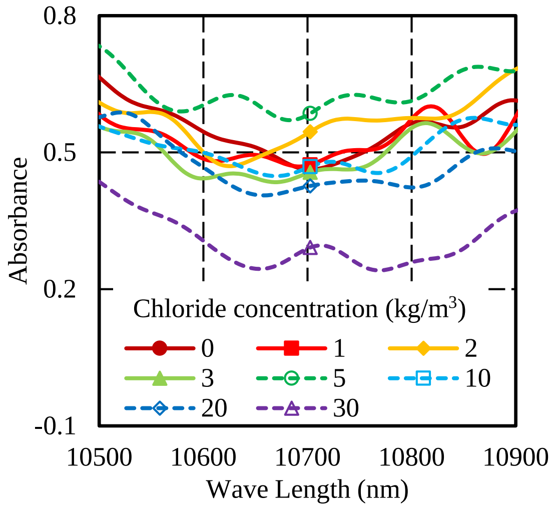

Fig.13 Absorbance data around 10700 nm

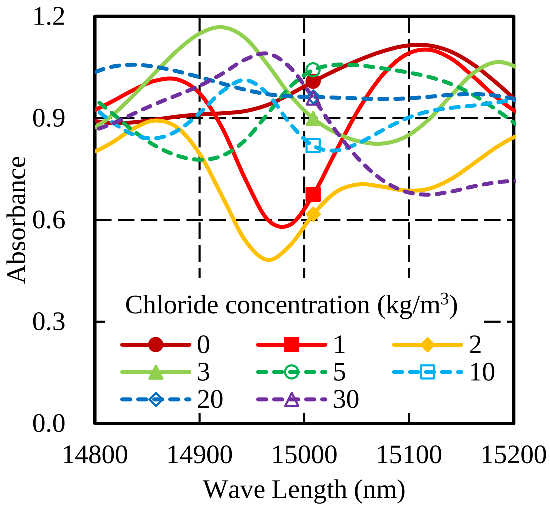

Fig.14 Absorbance data around 15000 nm

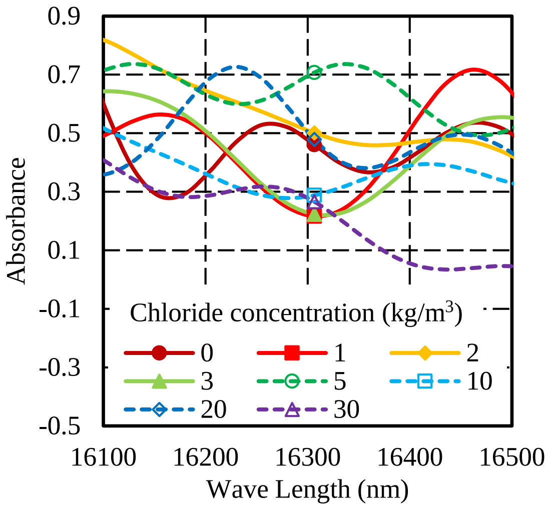

Fig.15 Absorbance data around 16300 nm

Next, the absorbance at 7339 nm, where the absolute value of loading was huge among the 7300 nm region, is negatively proportional to the chloride concentration (Fig.16). This suggests that 7339 nm is a characteristic wavelength that reflects the difference in chloride concentration.

On the other hand, in the study by Kanada et al., as shown in Fig.17, the difference between a straight line connecting two points that are not affected by other components in the wavelength band before and after the peak of the extracted spectrum is defined as the difference spectrum and calculated as shown in Eq.6 [11].

$$\Delta A_n = A_n - \left\{A_a + \frac{A_b - A_a}{\lambda_b - \lambda_a} \times (\lambda_n - \lambda_a)\right\} \qquad (6)$$

The difference spectrum is calculated by substituting the values obtained in this study into Eq.6, and the calculated results are shown in Fig.18. Further

$\boldsymbol{\lambda n}$, $\boldsymbol{\lambda a}$, and $\boldsymbol{\lambda b}$ are set to 7339 nm, 7222nm, and 7603 nm.

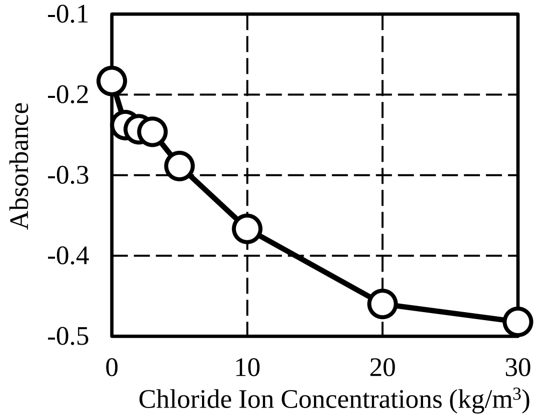

Fig.16 Relationship between absorbance and chloride concentration at 7339 nm

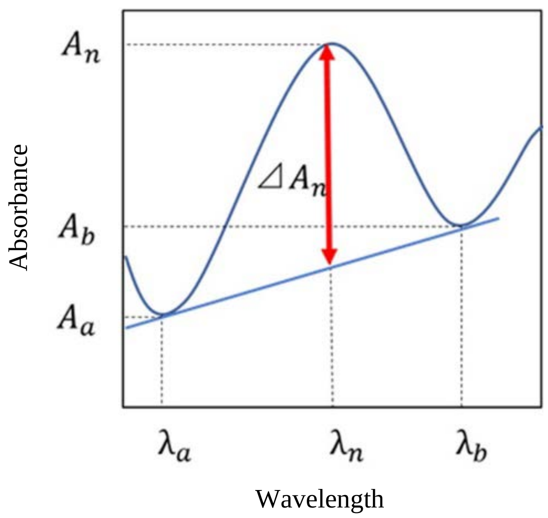

Fig.17 Concept of the difference spectrum

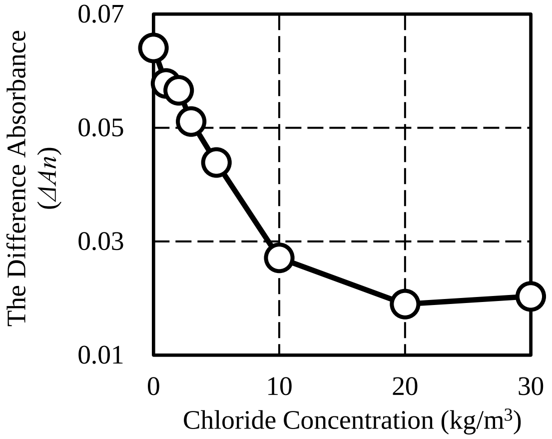

Fig.18 Relationship between calculated the difference spectrum and chloride concentration

Fig.16 shows that the absorbance decreases exponentially as the chloride concentration increases. Fig.18 shows the same trend as in Fig.15, suggesting that the absorbance converges at a chloride concentration of 20 kg/m^3. Therefore, it is suggested that it may not be possible to measure chloride concentrations above 20 kg/m^3.

8. MEASUREMENT BY THE COMPACT DEVICE

8.1 Experimental Method

A light source, a sample mounting apparatus, and the Compact Device were used for the measurements. The light source was a halogen lamp manufactured by Hawk Eye Technologies Co. The positional relationship is shown in Fig.19.

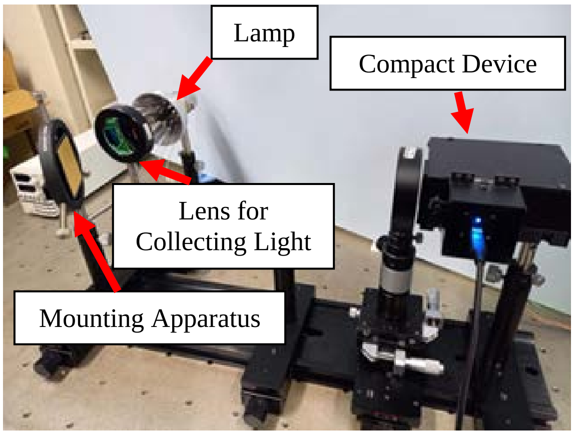

Fig.18 A scene of measurement using the Compact Device

The first step in the measurement procedure is to place an unwanted sample on the sample mounting apparatus and check and adjust whether sufficient luminance can be measured with the Compact Device. Once adequate illumination is obtained, the sample and gold plate are replaced to obtain a reference. Then, the measurement is carried out while replacing each sample. When setting up the samples, the measurement was carried out carefully so that the surface to be measured would not shift back and forth.

8.2 Measurement Results

First, from Fig.20, it can be seen that there was no defect in the measurement because the waveform in the wavelength range of 8000-14000 nm was similar to that of FTIR. However, the characteristic wavelength around 7300 nm, which was identified in the FTIR measurement, could not be confirmed by the compact device. The reason for this is that the measurement range of the compact device was between 8000 and 14000 nm. Therefore, there was quite a lot of noise as shown in Fig. 21, and no change in absorbance with chloride concentration was observed.

As a future issue, it is necessary to extend the measurement range so that the characteristic wavelength around 7300 nm identified in this study can be measured by the compact device. The measurement range can be extended by changing the lens.

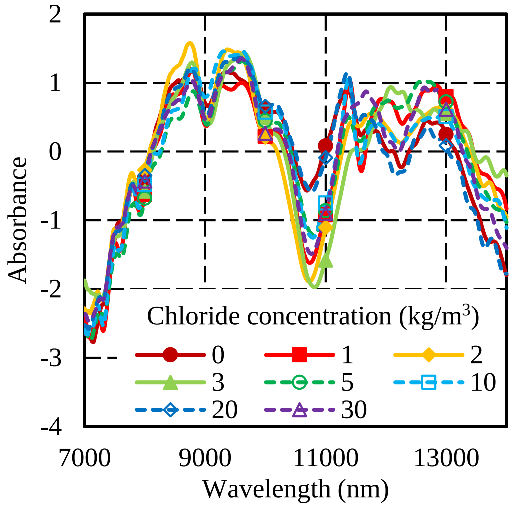

Fig.20 Spectral data acquired by the Compact Device after SNV processing

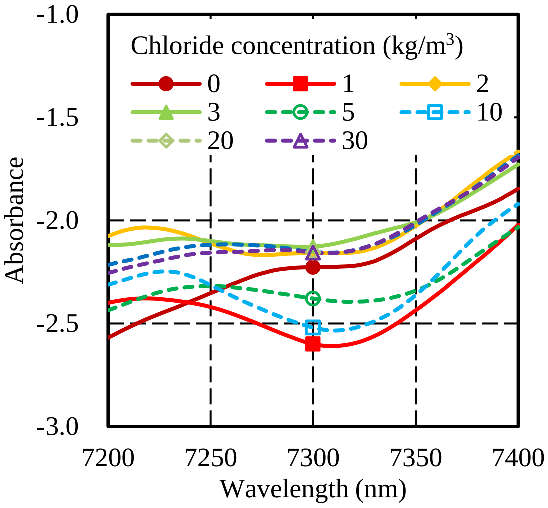

Fig.21 Spectral data around 7300 nm after SNV processing acquired by the Compact Device.

9. CONCLUSION

To develop and propose a chloride concentration detection system using mid-infrared spectroscopy as a new method for investigating chloride-induced damage to RC structures, this study reports on the middle infrared spectra of cement paste with sequentially changing chloride concentrations using mid-infrared spectroscopy.

As a result of FTIR measurement and multivariate analysis, it was confirmed that the wavelength reflecting the difference of chloride concentration existed around 7300nm. At 7339 nm, the correlation between chloride concentration and absorbance was strong. However, as a result of measurement using the Compact Device, it was impossible to measure around 7300 nm accurately, and the difference in chloride concentration could not be determined. In the future, it will be necessary to develop a compact device that can accurately measure around 7300 nm.

10. REFERENCES

[1] Saeki T., Shima T., and Nagataki S., Prediction of Chloride Penetration into Concrete by Equivalent Diffusion Coefficient, Proceedings of the Japan Concrete Institute, 20(2), 1998 pp. 859-864,

[2] Glass G. K., and Buenfeld N. R., The influence of chloride binding on the chloride-induced corrosion risk in reinforced concrete, Corrosion Science 42, 2000, pp. 329-344

[3] Ishikawa Y., Kanada H., Kato Y., and Uomoto T., Development of quantitative analysis of chloride content in concrete using the near-infrared method, Monthly journal of the Institute of Industrial Science, University of Tokyo, 58(3), 2006, pp. 281-284

[4] Nakajima Y., Shirane Y., Suenaga S., Hanya I., and Sakimura R., A Development on the Inspection System for Chloride Ion Content on the Concrete Surface Using Near-Infrared Spectrum and Its Application to the Maintenance of the RC Structures, Report of a technical research institute, Maeda Corporation, 57, 2016, pp.06

[5] Toda K., Nakamura Y., and Kurata T., System for Diagnosing Concrete Deterioration with Spectroscopic Analysis, IHI Engineering Review, 45(1) 2012, pp.31-36

[6] Watanabe A., Furukawa H., Miyamoto S., and Minagawa H., Nondestructive Chemical Analysis of Water and Chlorine Content in Cement Paste using Near-infrared Spectroscopy, Construction and Building Materials, 196(30), 2019, pp.95-104

[7] Wada K., Okazaki S., and Ishimaru I., Visualization of Chemical Composition and Chloride Ion Distribution by Novel NIR Imaging Spectroscopic System, Journal of the Imaging Society of Japan, 58(6), 2019, pp.664-650

[8] Sakakihara Y., Kabeyama Y., Hamada K., Okazaki S., Kanasaki K., Wada K., Ishimaru I. and Saito T., Development of Two-dimensional Imaging System of Surface Chloride Ion of Concrete Structure, Journal of Japan Society of Civil Engineers, Ser. B3 (Ocean Engineering), 75(2), 2019, pp. I_157-I_162

[9] Yamamoto N., Saito T., Ogawa S., and Ishimaru I., Middle Infrared (wavelength range: 8 μm-14 μm) 2-dimensional Spectroscopy (total weight with Electrical Controller: 1.7 kg, total cost: less than 10,000 USD) so-called hyperspectral camera for unmanned air vehicles like drones, Proc. SPIE 9840, Algorithms and Technologies for Multispectral, Hyperspectral, and Ultraspectral Imagery XXII, 2016

[10] Miyamoto K., Near-Infrared Spectroscopy III. Quantitative Analysis by Near-Infrared Spectroscopy, Journal of the spectroscopical research of Japan, 53(3), pp. 192-203

[11] Kanada H., Ishikawa Y. and Uomoto T., Application of Near-infrared Spectral Imaging for Componential Analysis of Concrete, Concrete Journal, Vol.44, No.4, pp.26-32, 2006